Aniket Mule[1,2,3,*], Bart Vermang[1,3,4], M. Sylvester[1,3,4], Guy Brammertz[4,5], Samaneh Ranjbar[1,3,6], Thomas Schnabel[7], Nikhil Gampa[1,3,8], Marc Meuris[4,5], Jef Poortmans[1,3,5]

[1] *imec – partner in Solliance, Kapeldreef 75, 3001 Leuven, Belgium*

[2] *Department of Mechanical and Process Engineering (D-MAVT), ETH Zurich, LEE K, Leonhardstrasse 21, 8092 Zurich, Switzerland*

[3] *Department of Electrical Engineering (ESAT), KU Leuven, Kasteelpark Arenberg 10, 3001 Heverlee, Belgium*

[4] *imec division IMOMEC - partner in Solliance, Wetenschapspark 1, 3590 Diepenbeek, Belgium*

[5] *Institute for Material Research (IMO) Hasselt University, Wetenschapspark 1, 3590 Diepenbeek, Belgium*

[6] *I3N - Departamento de Física, Universidade de Aveiro, Campus Universitário de Santiago, 3810-193 Aveiro, Portugal*

[7] *Zentrum für Sonnenenergie- und Wasserstoff-Forschung (ZSW), Industriestraße 6, 70565 Stuttgart, Germany*

[8] *École centrale de Lyon, 36 Avenue Guy de Collongue, 69134 Écully, France*

Effect of Different Alkali (Li, Na, K, Rb, Cs) Metals on $Cu_2ZnSnSe_4$ Solar Cells

Key: 88MT1

[*] Corresponding author; Tel: +41 788137368; E-mail: amule@student.ethz.ch

Effect of Different Alkali (Li, Na, K, Rb, Cs) Metals on $Cu_2ZnSnSe_4$ Solar Cells

Aniket Mule[1,2,3,*], Bart Vermang[1,3,4], M. Sylvester[1,3,4], Guy Brammertz[4,5], Samaneh Ranjbar[1,3,6], Thomas Schnabel[7], Nikhil Gampa[1,3,8], Marc Meuris[4,5], Jef Poortmans[1,3,5]

[1] *imec – partner in Solliance, Kapeldreef 75, 3001 Leuven, Belgium*

[2] *Department of Mechanical and Process Engineering (D-MAVT), ETH Zurich, LEE K, Leonhardstrasse 21, 8092 Zurich, Switzerland*

[3] *Department of Electrical Engineering (ESAT), KU Leuven, Kasteelpark Arenberg 10, 3001 Heverlee, Belgium*

[4] *imec division IMOMEC - partner in Solliance, Wetenschapspark 1, 3590 Diepenbeek, Belgium*

[5] *Institute for Material Research (IMO) Hasselt University, Wetenschapspark 1, 3590 Diepenbeek, Belgium*

[6] *I3N - Departamento de Física, Universidade de Aveiro, Campus Universitário de Santiago, 3810-193 Aveiro, Portugal*

[7] *Zentrum für Sonnenenergie- und Wasserstoff-Forschung (ZSW), Industriestraße 6, 70565 Stuttgart, Germany*

[8] *École centrale de Lyon, 36 Avenue Guy de Collongue, 69134 Écully, France*

[*] Corresponding author; Tel: +41 788137368; E-mail: amule@student.ethz.ch

Abstract

It is well established that the addition of sodium (Na) to chalcopyrite or kesterite based solar cells markedly increases the solar cell performance. In this work, we explore the effect of Na and other alkali metals like potassium (K), rubidium, caesium and lithium (Li) – on pure selenide $Cu_2ZnSnSe_4$ (CZTSe) solar cells. We demonstrate the deposition of alkali metals using spin coating on e-beam evaporated metal precursors. The stack of metal precursors with alkali layer was then selenised at high temperatures to obtain a good quality CZTSe absorber. The diffusion of alkali metals into the absorber layer was confirmed using glow discharge optical emission spectroscopy. Samples doped with Na or K have shown improvement in the open circuit voltage. A maximum power conversion efficiency of 8.3 % (without anti-reflection coating) and a top open circuit voltage 430 mV was achieved for combination of K and Na. Amongst the rest of alkali metals, Li looks the most promising dopant as far as optoelectronic properties are concerned.

Keywords:

CZTSe solar cell, alkali metals, spin coating, sodium, potassium, kesterites

1. Introduction

Thin film photovoltaics are gaining prominence with record efficiencies reaching up to 22.3% for $Cu(In,Ga)(S_xSe_{1-x})_2$ (hereafter referred as $CIGS_xSe_{1-x}$, $0 \leq x \leq 1$) [1]. However, the rapidly progressing display industry which uses indium and gallium will eventually limit the production of $CIGS_xSe_{1-x}$ due to the scarcity of these elements [2].

Kesterites like $Cu_2ZnSn(S_xSe_{1-x})_4$ (hereafter referred as $CZTS_xSe_{1-x}$, $0 \leq x \leq 1$) with their less toxic nature and more abundant elements are a promising alternative [2]. A record efficiency of 12.6 % was demonstrated [3], however, this is still far from the theoretical Shockley-

Queisser (SQ) limit of ~ 30 % [4]. Open circuit voltage (V_{oc}) deficit continues to be a key problem with the record cell reaching only 62.6 % of its SQ limit [2].

Addition of sodium (Na) to improve the performance of kesterite based cells has been inspired from the beneficial effects of Na doping in chalcopyrite based absorbers. Besides affecting the size of grains, Na also enhances the V_{oc} and fill factors of the devices, both these factors are largely sensitive to defects and traps [5-10]. Unlike $CIGS_xSe_{1-x}$, first principles calculations for $CZTS_xSe_{1-x}$ grain boundaries suggest that deep states do exist in the gap, which are expected to act as non-radiative recombination centres. [11]. Gershon et al. [12] recently demonstrated diffusion of Na to internal and external surfaces of the absorber in order to passivate them [13-15]. In addition, Na showed increase in the hole concentration in monocrystalline and polycrystalline $CZTS_xSe_{1-x}$ crystals [16, 17].

Potassium (K) is another alkali metal that has been incorporated into $CZTS_xSe_{1-x}$ / $CIGS_xSe_{1-x}$. In case of $CZTS_xSe_{1-x}$, presence of K suppresses the loss of tin and reduces the production of secondary phase zinc sulphide [18] resulting in lesser loss of zinc. K doping has shown to increase the crystallinity of $CZTS_xSe_{1-x}$ film and enhance the (112) preferred orientation.

In this study we aim to explore the effect of different alkali elements such as lithium (Li), sodium (Na), potassium (K), rubidium (Rb) and caesium (Cs) – on pure selenide CZTSe ($CZTS_xSe_{1-x}$, x=0) solar cells. The inclusion of alkali elements was done by spin coating followed by selenisation at high temperature leading to the formation of the CZTSe absorber containing the alkali atoms. The purpose of this study is to give an overview of the impact of different alkali elements on the optoelectronic and electrical properties of CZTSe solar cells. We believe, the results of this study will be helpful to initiate a detailed investigation into alkali elements that have a potential to improve the CZTSe devices.

2. Experimental Details

2.1 Fabrication

A 3 mm thick soda lime glass sputtered with 500 nm molybdenum (Mo) was purchased from Guardian Industries. Two different kinds of substrates were used: I) with a 200 nm intermediate barrier layer of Silicon Oxynitride between soda lime glass and Mo to prevent in-diffusion of alkali metals (hereafter referred to as SLG-B) II) without any barrier layer (hereafter referred to as SLG).

Tin, zinc and copper were deposited on the aforementioned substrates with thickness of 215, 95 and 110 nm respectively, using Pfeiffer e-beam evaporation. Before selenisation, alkali metals were spin coated on the stack of metal precursors. Fluoride salts of alkali metals were dissolved in water with appropriate concentrations (lithium fluoride (LiF) = 0.1 M, sodium fluoride (NaF) = 0.1 M, potassium fluoride (KF) = 0.1 M, rubidium fluoride (RbF) = 0.01 M, caesium fluoride (CsF) = 0.005 M) and this was used as a solution for spin coating. The speed for the spin coater was set to 1000 rpm, with an acceleration of 1000 rpm/s^2. The samples were spun for 6 minutes.

The stacked metal layers are then selenized to form absorber in one of the following furnaces:

1. In hydrogen selenide (H_2Se) atmosphere as demonstrated by Brammertz et al.[19]. This was the preferred method of selenisation. Hereafter it is referred to as Annealsys.

2. In selenium atmosphere as demonstrated by Zaghi et al.[20]. This method was used to limit contamination of the Annealsys furnace by Rb, Cs, and Li. Hereafter this method is referred to as Quartz tube based Rapid Thermal annealing Process (QRTP).

These absorber layers were etched in 5 % potassium cyanide (KCN) solution for 2 minutes. The devices were completed by successive chemical bath deposition of cadmium sulfide (50 nm), sputtering of intrinsic zinc oxide (ZnO) (120 nm) and aluminium doped ZnO (280 nm). A top contact of nickel/aluminium was deposited for devices selenised only in Annealsys. For samples selenised in QRTP furnace, no top contact was deposited. Solar cells were isolated by needle scribing of the devices. The area of cells was 0.5 cm^2 and 0.09 cm^2 for devices selenised in Annealsys and QRTP respectively.

All the devices reported here were annealed in air for 1 hour at 200°C. The effect of annealing was not clearly established. The electrical properties of solar cells before annealing were compared with devices after annealing. If the electrical properties improved then the properties after annealing are reported (See Table 1). Similarly, if the device performance degraded after annealing then the properties before annealing have been reported (See Table 1). A detailed study on the effect of annealing is beyond the scope of this study. An overview of the sample set is given in Table 1.

2.2 Characterisation

The processed solar cells were analysed using current density-voltage (J-V, 2600 Source meter, Keithley) measurements performed under a solar simulator system (Model 6143, Oriel) using an AM1.5G spectrum with an illumination density of 1000 W/m^2.

Time-resolved photoluminescence (TRPL) measurements were acquired with a Hamamatsu C12132 (Hamamatsu Photonics, Hamamatsu, Japan) near-infrared compact fluorescence lifetime measurement system. An area of 3-mm diameter with an average laser power of 1 mW was illuminated on the absorber layers with a 15 kHz, 1.2 ns pulsed 532 nm laser for the minority charge carrier lifetime measurements. All the measurements were done at room temperature.

The distribution of the alkali elements Na and K in the absorber were measured by a Horiba Scientific GD-Profiler 2 glow discharge optical emission spectrometer (GDOES) which is operated in radio frequency mode at powers of 26 W and argon pressures of 500 Pa. The measurement spot has a diameter of 4 mm and a depth-resolution within the absorber of about 60 nm is achieved, comparable with other thin-film analytical methods like secondary ion mass spectrometry [10].

The external quantum efficiency (EQE) has been measured at room temperature using a laboratory-built system with a grating monochromator-based dual-beam setup under chopped light from a xenon lamp.

3. Results and Discussion

The results are discussed in three sections. The first section describes the samples selenised in Annealsys. The second section deals with the samples selenised in QRTP furnace. The third and final section gives an overview of statistics involved in the measurements of optoelectronic properties.

3.1 Sample selenised in Annealsys

This section deals with studies carried out on solar cells whose absorber layers were synthesised in Annealsys furnace. Na and K were the only alkali elements used for doping. The absorbers doped with alkali elements were fabricated only on SLG-B substrates. The reference samples containing a CZTSe absorber layer without any external alkali dopant on SLG substrate (hereafter SLG Reference sample) and SLG-B substrate (hereafter SLG-B reference sample) were also analysed.

Figure 1 shows GDOES measurements carried out on alkali-doped and reference samples. The samples used for GDOES studies were processed only till the absorber layer. Therefore,

a sputtering time of 0 s indicates the surface of the absorber. The SLG-B reference samples show very low Na/K signal indicating the effectiveness of barrier. The SLG reference samples however had a very high sodium signal at front and back interfaces. This indicates a significant sodium in-diffusion from the soda lime glass into the absorber layer. The samples doped with sodium or potassium showed a similar trend of accumulation at the front or back interfaces. The strength of signal was dependent on concentration and the type of alkali solution used for spin coating. For same set of concentrations, the Na signal was stronger compared to K indicating easier diffusion of Na as compared to K. The strength of signal for Na was proportional to concentration of NaF solution used for spin coating.

The GDOES results prove that the alkali metals deposited using spin coater have diffused into the absorber. The dependence of the strength of signal on concentration of alkali metal solution demonstrates the systematic nature of our technique. The accumulation of Na and K at front or back interfaces is in good agreement with the literature [12-15]. However, a complete solar cell fabrication involves KCN etching and water rinsing steps. The excess of Na and K present at the front interface will then be washed away due to high solubility of fluoride salts in water [21].

Figure 2 (a) shows the minority carrier lifetime of various samples. Doping the absorber layer with alkali elements results in the improvement of lifetime of minority carriers. The samples doped with combination of Na and K showed the highest lifetime. This suggests that combination of Na and K helps in increasing minority carrier lifetime indicating the improvement in collection of charge carriers.

The electrical parameters of the cells fabricated are given in Table 2. A top power conversion efficiency (PCE) of 8.3 % and a top V_{oc} of 430 mV was achieved for samples doped with

combination of Na and K without use of any anti-reflection coating. The samples doped with alkali metals show an increase in V_{oc} over the SLG-B reference samples.

The J-V curve for devices doped with a combination of Na and K is given in Figure 3 (a). It is compared with a reference SLG-B sample. An appreciable increase in all the electrical characteristics was noticed when samples were doped with combination of Na and K (NaF:KF = 2:1) in comparison to the reference samples. The J-V results were in good agreement with our EQE results (Figure 3 (b)). The EQE measurements showed an increase in collection of charge carriers at all wavelengths. This improvement of electrical properties for doping combination of Na and K has been previously observed for $CIGS_xSe_{1-x}$ [22]. Before concluding with this section, we would like to note that the device with the highest power conversion efficiency had the longest lifetime amongst absorbers fabricated on SLG-B substrates.

3.2 Sample selenised in QRTP

This section deals with studies carried out on solar cells whose absorber layers were synthesised in QRTP furnace. All the alkali elements i.e Li, Na, K, Rb, and Cs were individually used for doping. The absorbers doped individually with Na and K were fabricated only on the SLG-B substrates. However, the absorbers doped individually with Li, Rb, and Cs were fabricated on both the substrates. The reference samples on both substrates were also analysed.

Figures 2 (b) and 2 (c) show the minority carrier lifetime in the CZTSe absorbers doped with different elements on SLG-B and SLG substrates respectively. For SLG-B substrates, samples doped with Li and Cs showed the highest lifetime (Figure 2 (b)). For SLG substrates, samples doped with Li showed the highest lifetime (Figure 2 (c)).

The aforementioned results show that alkali metals improves the lifetime of minority carrier as in the case of samples selenised in Annealsys furnace. Li and Cs, strictly in perspective of optoelectronic properties, seem to be promising dopants.

For samples selenised in QRTP, the absolute values of PCE are relatively low as compared to samples selenised in Annealsys. A plot showing relative change of PCE with respect to a reference solar cell on same substrate is shown in Figure 4. For the solar cells processed on SLG-B substrates (green squares in Figure 4), the largest increase in PCE was obtained for samples doped with Na. The samples doped with Li, Rb, and Cs do not show any significant improvement over the reference samples. For the solar cells which were processed on SLG substrates (red circles in Figure 4), we note an increase of 30-40% in efficiency for samples doped with Cs and Li over the reference cells. Therefore, a mixture of Na and Li or Na and Cs could be a topic of interest for future experiments.

For the similar doping conditions, solar cells selenised in QRTP furnace showed relatively low efficiencies compared to solar cells selenised in Annealsys furnace which could be attributed to the selenisation-specific problems. Initial scanning electron micrographs and visual inspections of absorbers selenised in QRTP indicated a thicker $MoSe_2$ layer. A thicker $MoSe_2$ could indicate higher interaction between CZTSe and Mo leading to the decomposition of CZTSe as explained by Scragg et al. [23]. The addition of an inhibitor layer like titanium nitride between Mo and $CZTS_xSe_{1-x}$ [24] could readily solve this problem. Since the main objective of this study was to explore the effect of alkali elements in an empirical manner, the detailed investigation into this is beyond the scope of this study.

3.3 Statistics in measurement of optoelectronic properties

This section gives an overview of statistics in measurement of optoelectronic properties in our studies. The variation in minority carrier lifetime and photoluminescence (PL) peak of devices with similar doping conditions but different experimental trials is discussed here.

A standard TRPL spectra of the SLG and SLG-B reference samples is shown in Figure 5 (a). The extracted minority carrier lifetime from the spectra shows that a substrate without a barrier layer has a higher lifetime as compared to a substrate with a barrier layer. This trend of SLG reference samples having higher lifetime than SLG-B reference samples was consistent with all selenisation cycles. However, the values were not exactly reproducible. Therefore we decided to use reference samples for all our cycles so that we can have a valid comparison of lifetime between different trials. This variation of lifetime for reference samples selenised in Annealsys and QRTP furnace can be seen in Figure 5 (b).

The peak position of PL signal had wide range of variation for samples selenised in Annealsys. In contrast, the PL spectra was very reproducible for samples selenised in QRTP furnace, as is shown in Figure 6. An ideal CZTSe absorber would have a bandgap of 1 eV. For samples selenised in QRTP furnace, the PL spectra shows that the deposited absorber has bandgap of ~ 1 eV (1240 nm). However, the selenisation in Annealsys resulted in the formation of a lower bandgap (< 1 eV) absorber.

The reason behind the large distribution in peak position of PL spectra and variation of lifetime in Annealsys could be the large susceptor area over which samples were being selenised. This resulted in non-uniform flow of H_2Se and formation of temperature gradient across the susceptor. Although the PL spectra of the samples selenised in QRTP furnace was reproducible, the rapid selenisation of Mo in QRTP resulted in thicker $MoSe_2$ as discussed in the previous section.

4. Conclusion

Spin coating was employed as a method to incorporate the alkali metals into the CZTSe absorber in a systematic manner. The absorbers doped with alkali metals showed an increase in lifetime of minority carriers as compared to SLG-B reference samples. A top V_{oc} of 430 mV and PCE as high as 8.3 % (without anti-reflection coating) was achieved by doping the absorber layer with a combination of sodium and potassium. This is in good agreement with the improved charge collection at all wavelengths as indicated by the EQE measurements. Amongst the other alkali metals, Li seems to be the most promising dopant for a kesterite based absorber considering the optoelectronic properties. Although the electrical characteristics don't stand out individually for devices doped with Li or Cs, our findings suggest that a combination of Li and Na or Cs and Na could be a subject of interest for future studies.

Acknowledgements

This project has received funding from the European Union's Horizon 2020 research and innovation program under grant agreement No 640868. This research is partially funded by the Flemish government, Department Economy, Science and innovation. B. Vermang acknowledges the financial support of the Flemish Research Foundation FWO (mandate 12O4215N).

References

[1] K. Maraun, Solar Frontier Achieves World Record Thin-Film Solar Cell Efficiency: 22.3%. http://www.solar-frontier.com/eng/news/2015/C051171.html , 2015 (accessed 08.12.2015).

[2] X. Liu, Y. Feng, H. Cui, F. Liu, X. Hao, G. Conibeer, D.B. Mitzi, M. Green, The current status and future prospects of kesterite solar cells: a brief review, Prog. Photovolt.: Res. Appl. 24 (2016) 879-898.

[3] W. Wang, M.T. Winkler, O. Gunawan, T. Gokmen, T.K. Todorov, Y. Zhu, D.B. Mitzi, Device Characteristics of CZTSSe Thin-Film Solar Cells with 12.6% Efficiency, Adv. Energy Mater. 4 (2014) 1301465.

[4] W. Shockley, H.J. Queisser, Detailed Balance Limit of Efficiency of p- n Junction Solar Cells, J. Appl. Phys. 32 (1961) 510-519.

[5] P.T. Erslev, J.W. Lee, W.N. Shafarman, J.D. Cohen, The influence of Na on metastable defect kinetics in CIGS materials, Thin Solid Films 517 (2009) 2277-2281.

[6] J.V. Li, D. Kuciauskas, M.R. Young, I.L. Repins, Effects of sodium incorporation in Co-evaporated $Cu_2ZnSnSe_4$ thin-film solar cells, Appl. Phys. Lett. 102 (2013) 163905.

[7] T. Nakada, D. Iga, H. Ohbo, A. Kunioka, Effects of sodium on Cu(In, Ga)Se_2-based thin films and solar cells, Jpn. J. Appl. Phys. 36 (1997) 732.

[8] H. Zhou, T.-B. Song, W.-C. Hsu, S. Luo, S. Ye, H.-S. Duan, C.-J. Hsu, W. Yang, Y. Yang, Rational defect passivation of $Cu_2ZnSn(S, Se)_4$ photovoltaics with solution-processed Cu_2ZnSnS_4: Na nanocrystals, J. Am. Chem. Soc. 135 (2013) 15998-16001.

[9] T. Nakada, Invited Paper: CIGS-based thin film solar cells and modules: Unique material properties, Electron. Mater. Lett. 8 (2012) 179-185.

[10] T. Abzieher, T. Schnabel, M. Hetterich, M. Powalla, E. Ahlswede, Source and effects of sodium in solution-processed kesterite solar cells, Phys. Status Solidi (a) 213 (2016) 1039-

1049.

[11] J. Li, D.B. Mitzi, V.B. Shenoy, Structure and electronic properties of grain boundaries in earth-abundant photovoltaic absorber $Cu_2ZnSnSe_4$, ACS nano 5 (2011) 8613-8619.

[12] T. Gershon, B. Shin, N. Bojarczuk, M. Hopstaken, D.B. Mitzi, S. Guha, The Role of Sodium as a Surfactant and Suppressor of Non-Radiative Recombination at Internal Surfaces in Cu_2ZnSnS_4, Adv. Energy Mater. 5 (2015) 1400849.

[13] L. Kronik, D. Cahen, H.W. Schock, Effects of sodium on polycrystalline Cu(In, Ga)Se_2 and its solar cell performance, Adv. Mater. 10 (1998) 31-36.

[14] D.W. Niles, M. Al-Jassim, K. Fiamanathan, Direct observation of Na and O impurities at grain surfaces of $CuInSe_2$, J. Vac. Sci. Technol. A 17 (1999) 291-296.

[15] R. Haight, X. Shao, W. Wang, D.B. Mitzi, Electronic and elemental properties of the $Cu_2ZnSn(S, Se)_4$ surface and grain boundaries, Appl. Phys. Lett. 104 (2014) 033902.

[16] A. Nagaoka, H. Miyake, T. Taniyama, K. Kakimoto, Y. Nose, M.A. Scarpulla, K. Yoshino, Effects of sodium on electrical properties in Cu_2ZnSnS_4 single crystal, Appl. Phys. Lett. 104 (2014) 152101.

[17] T. Prabhakar, N. Jampana, Effect of sodium diffusion on the structural and electrical properties of Cu_2ZnSnS_4 thin films, Sol. Energy Mater. Sol. Cells 95 (2011) 1001-1004.

[18] Z. Tong, C. Yan, Z. Su, F. Zeng, J. Yang, Y. Li, L. Jiang, Y. Lai, F. Liu, Effects of potassium doping on solution processed kesterite Cu_2ZnSnS_4 thin film solar cells, Appl. Phys. Lett. 105 (2014) 223903.

[19] G. Brammertz, S. Oueslati, M. Buffiere, J. Bekaert, H. El Anzeery, K. Ben Messaoud, S. Sahayaraj, T. Nuytten, C. Koble, M. Meuris, Investigation of Properties Limiting Efficiency in $Cu_2ZnSnSe_4$-Based Solar Cells, IEEE J. Photovolt. 5 (2015) 649-655.

[20] A.E. Zaghi, M. Buffière, G. Brammertz, N. Lenaers, M. Meuris, J. Poortmans, J. Vleugels, Selenization of printed Cu–In–Se alloy nanopowder layers for fabrication of $CuInSe_2$ thin film solar cells, Thin Solid Films 582 (2015) 18-22.

[21] C.M. Sutter-Fella, Solution-processed kesterite absorbers for thin film solar cells, Diss., Eidgenössische Technische Hochschule ETH Zürich, Nr. 21883, 2014.

[22] A. Chirila, P. Reinhard, F. Pianezzi, P. Bloesch, A.R. Uhl, C. Fella, L. Kranz, D. Keller, C. Gretener, H. Hagendorfer, D. Jaeger, R. Erni, S. Nishiwaki, S. Buecheler, A.N. Tiwari, Potassium-induced surface modification of $Cu(In,Ga)Se_2$ thin films for high-efficiency solar cells, Nat. Mater. 12 (2013) 1107-1111.

[23] J.J. Scragg, J.T. Wätjen, M. Edoff, T. Ericson, T. Kubart, C. Platzer-Björkman, A Detrimental Reaction at the Molybdenum Back Contact in $Cu_2ZnSn(S,Se)_4$ Thin-Film Solar Cells, J. Am. Chem. Soc. 134 (2012) 19330-19333.

[24] J.J. Scragg, T. Kubart, J.T. Wätjen, T. Ericson, M.K. Linnarsson, C. Platzer-Björkman, Effects of Back Contact Instability on Cu_2ZnSnS_4 Devices and Processes, Chem. Mater. 25 (2013) 3162-3171.

Sample Set	Substrates	Selenisation Furnace	Concentration of Alkali Salts in Water	Reported Electrical Characteristics After (A) / Before (B) Annealing
	SLG-B	QRTP	LiF - 0.1 M	A
			NaF - 0.1 M	
			KF - 0.1 M	
			RbF - 0.01 M	
			CsF - 0.005 M	
			Reference	
		Annealsys	NaF - 0.1 M	A
			KF - 0.1 M	B
			NaF:KF (2:1)	A
			Reference	
	SLG	QRTP	LiF - 0.1 M	A
			RbF - 0.01 M	
			CsF - 0.005 M	
			Reference	
		Annealsys	Reference	

Table 1: Overview of the sample set used in the study. The columns in the table highlight the differences in substrates and fabrication process used for processing of the solar cell. A front contact of Ni/Al was deposited for all the samples selenised in Annealsys furnace . No front contact was deposited for samples selenised in QRTP furnace.

	NaF (0.1 M)	KF (0.1 M)	NaF + KF (NaF: KF = 2:1)	SLG-B Reference	SLG Reference
J_{sc} (mA/cm^2)	33.1 ± 1.5	28.1 ± 1.7	34.6 ± 2	31.8 ± 2.4	26.9 ± 3.1
V_{oc} (mV)	372 ± 10	364 ± 4	389 ± 6	336 ± 25	385 ± 28
FF (%)	48 ± 1	46 ± 2	57 ± 1	49 ± 6	50 ± 2
Efficiency (%)	5.9 ± 0.4	4.7 ± 0.3	7.7 ± 0.5	5.3 ± 1	5.2 ± 1.1
Best Efficiency (%)	6.1	5.6	8.3	5.3	6.7

Table 2: Electrical characteristics obtained from J-V measurements carried out on 0.5 cm^2 CZTSe solar cells. The SLG-B/Mo/CZT were coated with different alkali element using spin coater and selenised in Annealsys furnace to fabricate the absorber layer. Reference SLG/Mo/CZT or SLG-B/Mo/CZT samples were directly selenised in Annealsys furnace. The average short circuit current (J_{sc}), open circuit voltage (V_{oc}), fill factor (FF), and cell efficiency (%), and best efficiency (%) obtained with particular doping combination are given.

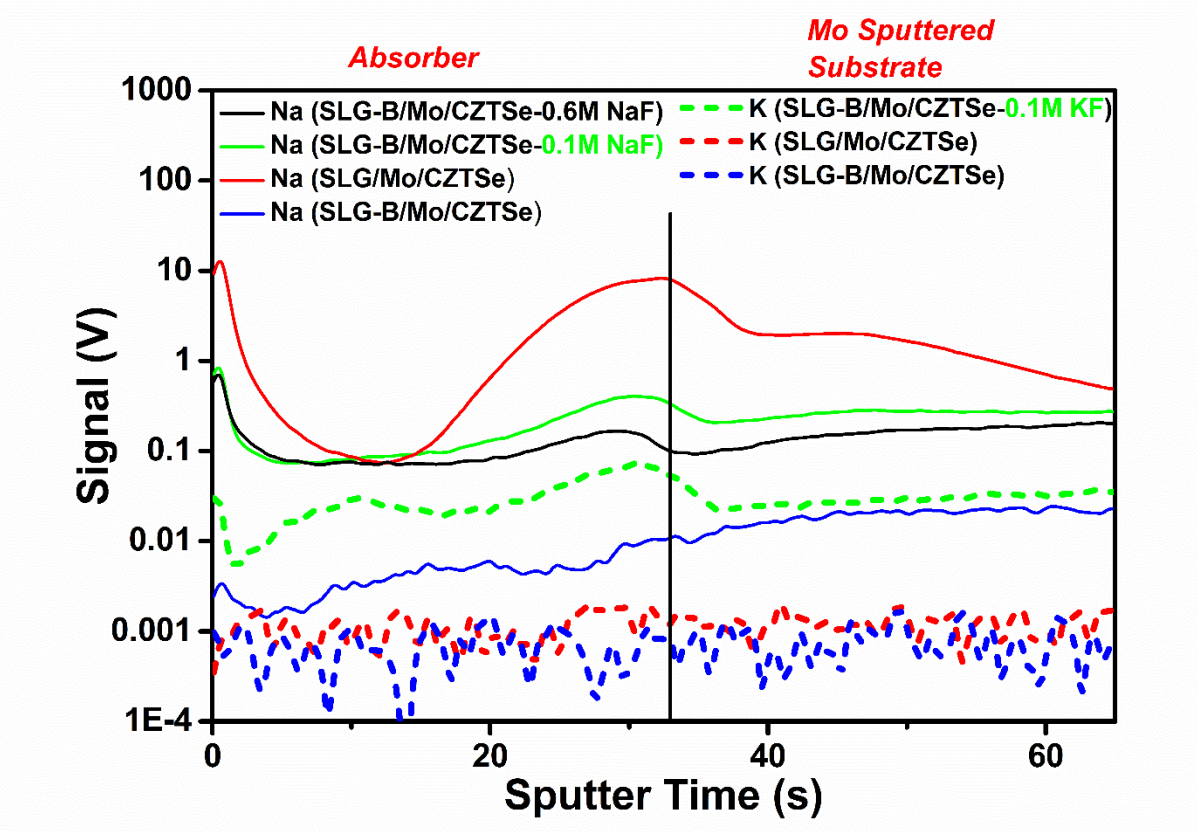

Figure 1: GDOES measurements done on SLG-B/Mo/CZTSe, SLG/Mo/CZTSe, SLG-B/Mo/CZTSe-NaF and SLG-B/Mo/CZTSe-KF samples. Sputter time = 0 s indicates the top surface of the CZTSe absorber layer. The absorbers were synthesised in Annealsys.

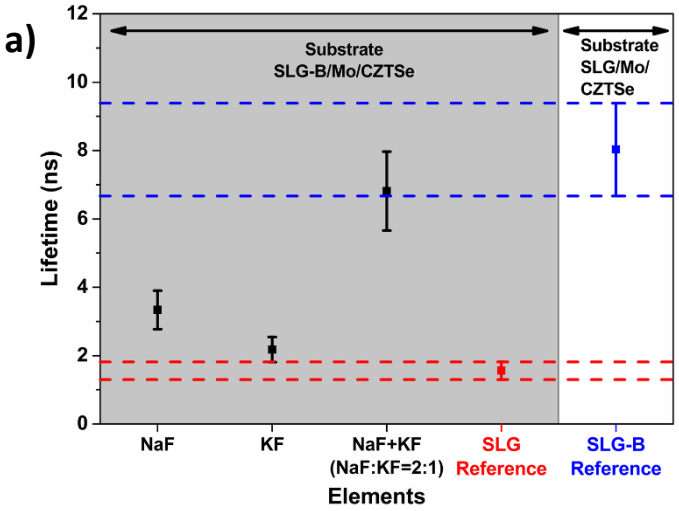

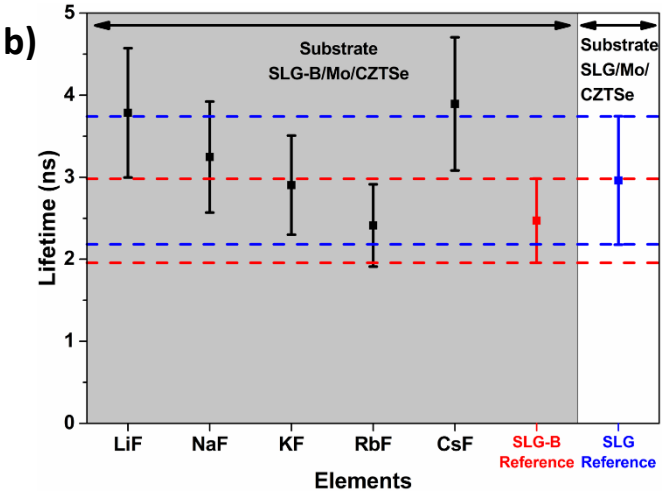

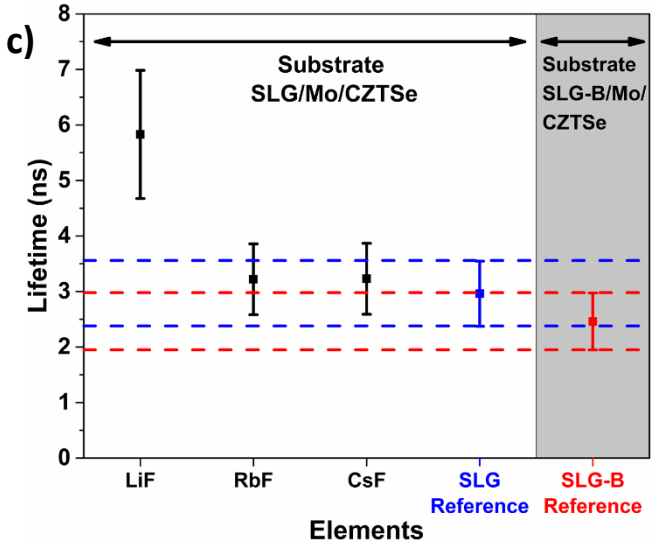

Figure 2: Average minority carrier lifetime values obtained from TRPL measurements (a) on SLG-B/Mo/CZTSe samples selenised in Annealsys Furnace. (b) on SLG-B/Mo/CZTSe samples selenised in QRTP Furnace. (c) on SLG/Mo/CZTSe samples selenised in QRTP

furnace. The x-axis indicate fluoride salts of alkali metals used for doping of absorber layers. The red and blue dotted lines indicate the standard deviation in the minority carrier lifetime of reference samples (CZTSe absorbers without any external doping of alkali metals) over different selenisation runs. The area shaded by grey colour show the minority carrier lifetime of samples selenised on SLG-B substrates. The unshaded area shows the minority carrier lifetime of samples selenised on SLG substrates.

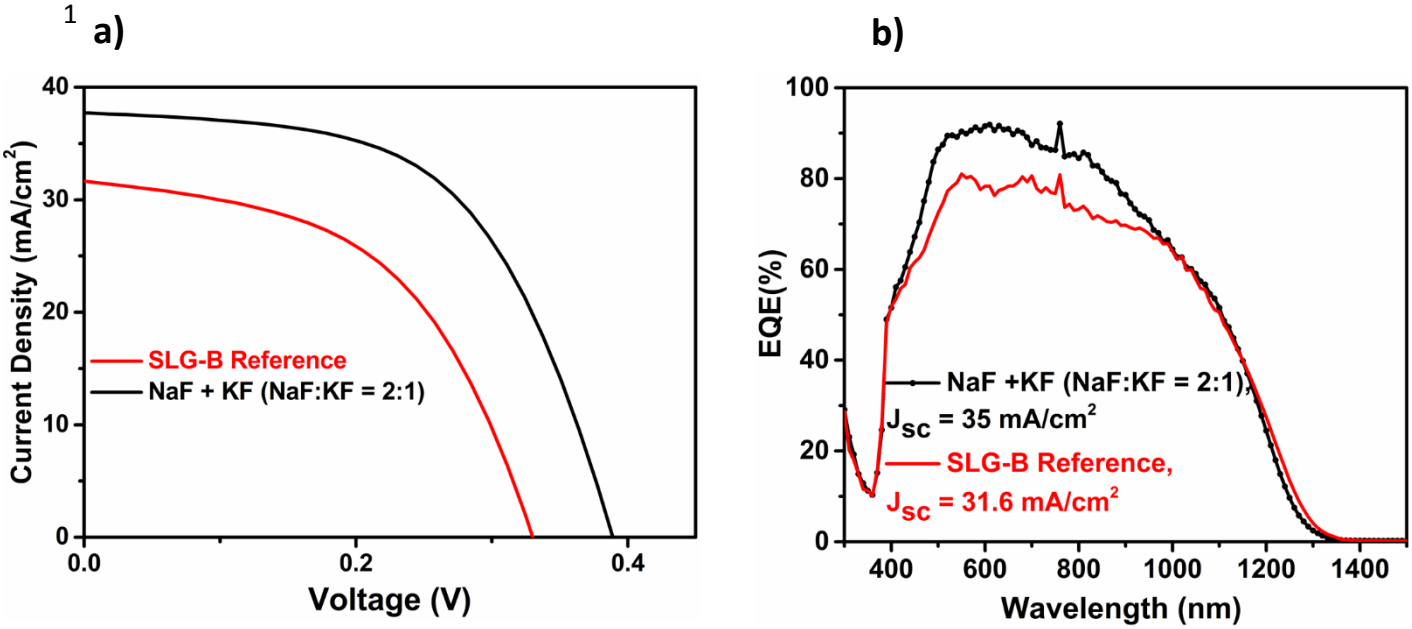

Figure 3: a) Current Density vs Voltage (J-V) measurements and b) EQE measurements carried out for devices doped with a combination of NaF and KF with a ratio NaF:KF = 2:1 in comparison with reference SLG-B sample. The substrates were selenised in Annealsys furnace. The average short circuit current density (J_{sc}) was calculated from the EQE measurements and compared with the J-V results.

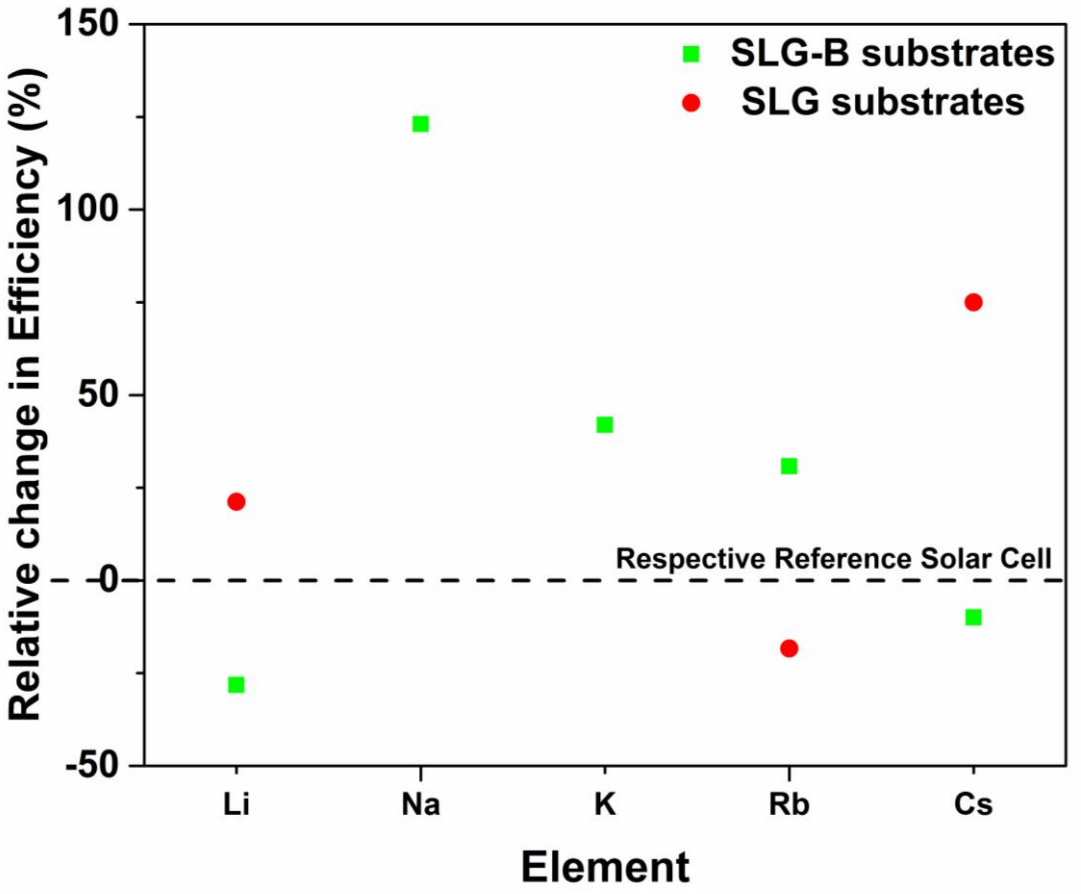

Figure 4: Relative change in PCE of completely processed solar cells doped with different alkali metals on SLG-B substrates (Green Squares) and SLG substrates (Red Circles) in comparison to reference solar cells (Black Dashed Line) on same substrate. The substrates were selenised in QRTP furnace.

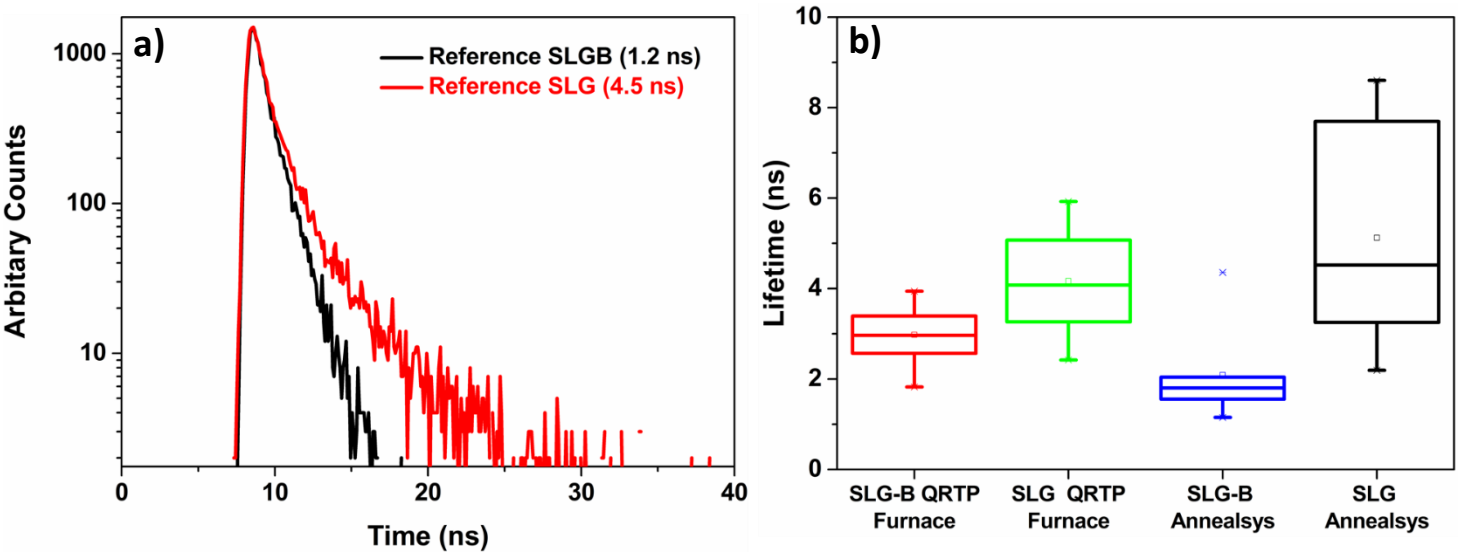

Figure 5: (a) Standard time-resolved PL spectra of SLG and SLG-B reference samples. (b) Box plot showing the variation of lifetime of SLG and SLG-B reference samples.

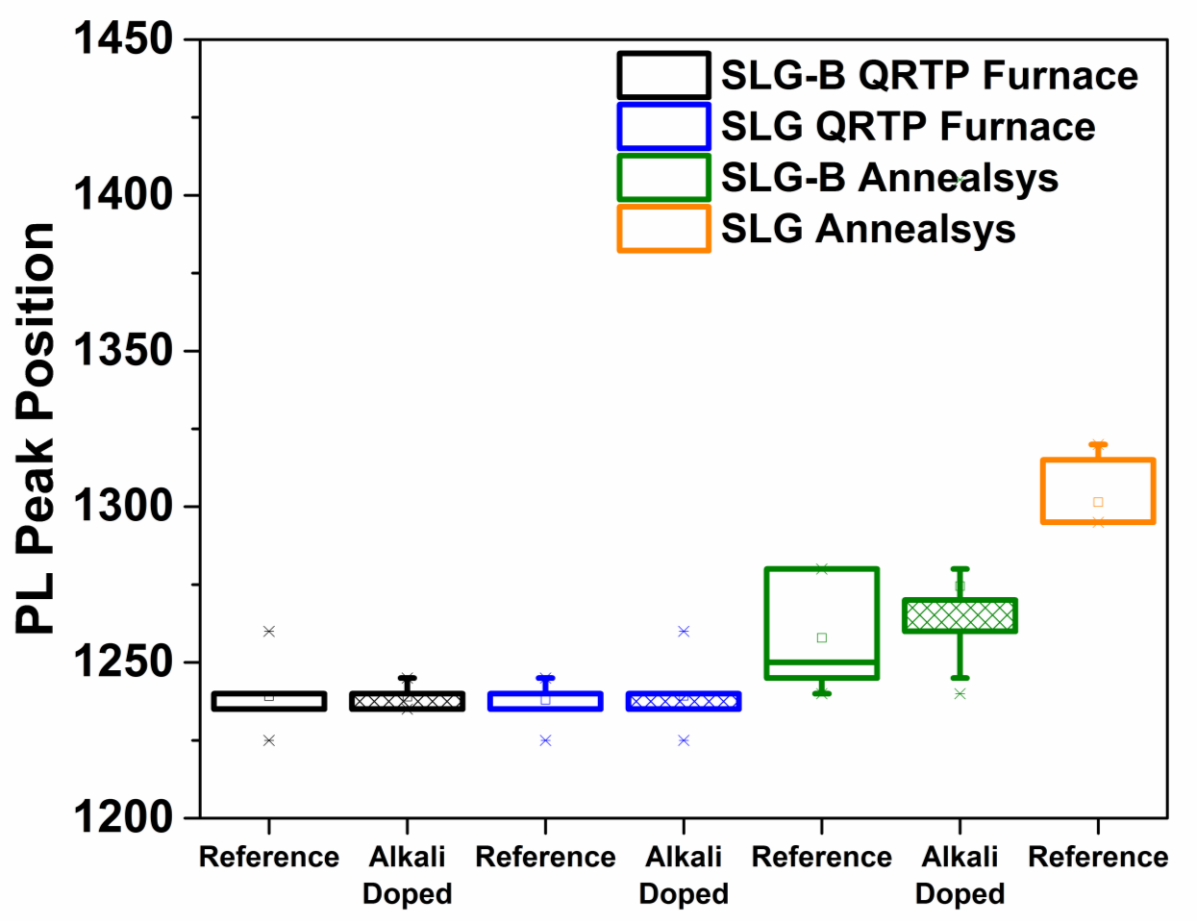

Figure 6: Box plot showing the variation of peak position of PL for reference samples and alkali doped samples selenised in different furnaces. The colour of the box indicates the type of substrate and the furnace used. Empty boxes indicate the variation of position for PL peak in reference samples (CZTSe absorbers without any external doping of alkali metals). Patterned boxes indicate the variation of position for PL peak in alkali-doped CZTSe absorbers. Each box for alkali doped samples includes all samples doped with either of the alkali elements (Li, Na, K, Rb, Cs) selenised in same furnace and same substrate. Data from at least 7 trials (= 7 different selenisation runs) for every type of sample was used while calculating the statistics.